Pharm Res (2015) 32:2983–2994
DOI 10.1007/s11095-015-1680-8

RESEARCH PAPER

Preparation and Evaluation of Multiple Nanoemulsions Containing Gadolinium (III) Chelate as a Potential Magnetic Resonance Imaging (MRI) Contrast Agent

Estelle Sigward[1] • Yohann Corvis[1] • Bich-Thuy Doan[1] • Kadri Kindsiko[1] • Johanne Seguin[1] • Daniel Scherman[1] • Denis Brossard[1] • Nathalie Mignet[1] • Philippe Espeau[1] • Sylvie Crauste-Manciet[1,2]

Received: 8 December 2014 / Accepted: 18 March 2015 / Published online: 25 March 2015
© Springer Science+Business Media New York 2015

ABSTRACT

Purpose The objective was to develop, characterize and assess the potentiality of $W_1/O/W_2$ self-emulsifying multiple nanoemulsions to enhance signal/noise ratio for Magnetic Resonance Imaging (MRI).

Methods For this purpose, a new formulation, was designed for encapsulation efficiency and stability. Various methods were used to characterize encapsulation efficiency ,in particular calorimetric methods (Differential Scanning Calorimetry (DSC), thermogravimetry analysis) and ultrafiltration. MRI *in vitro* relaxivities were assessed on loaded DTPA-Gd multiple nanoemulsions.

Results Characterization of the formulation, in particular of encapsulation efficiency was a challenge due to interactions found with ultrafiltration method. Thanks to the specifically developed DSC protocol, we were able to confirm the formation of multiple nanoemulsions, differentiate loaded from unloaded nanoemulsions and measure the encapsulation efficiency which was found to be quite high with a 68% of drug loaded. Relaxivity studies showed that the self-emulsifying W/O/W nanoemulsions were positive contrast agents, exhibiting higher relaxivities than those of the DTPA-Gd solution taken as a reference.

Conclusion New self-emulsifying multiple nanoemulsions that were able to load satisfactory amounts of contrasting agent were successfully developed as potential MRI contrasting agents. A specific DSC protocol was needed to be developed to characterize these complex systems as it would be useful to develop these self-formation formulations.

✉ Sylvie Crauste-Manciet
sylvie.crauste-manciet@chu-bordeaux.fr

[1] U1022 INSERM, UMR8258 CNRS, Unité de Technologies Chimiques et Biologiques pour la Santé, Chimie ParisTech, Faculty of PharmacyParis Descartes University, Sorbone Paris Cité, 75006 Paris, France

[2] ARNA Laboratory, ChemBioMed U869, Pharmaceutical Science Faculty University of Bordeaux, 146 rue Leo Saignat, 33000 Bordeaux, France

KEY WORDS differential scanning calorimetry · magnetic resonance imaging · multiple nanoemulsions · self-emulsifying · ultrafiltration

ABBREVIATIONS

DLS	Dynamic Light Scattering
DSC	Differential Scanning Calorimetry
DTPA-Eu	Diethylene tri-amine penta acetic acid—Europium
DTPA-Gd	Diethylene tri-amine penta acetic acid—Gadolinium
E.E	Encapsulation efficiency
HSA	Human Serum Albumin
ICP-AES	Inductively Coupled Plasma Absorption Emission Spectroscopy
ICP-MS	Inductively Coupled Plasma Mass Spectrometry
MDS	Mean Droplet Size
MRI	Magnetic Resonance Imaging
PDI	Polydispersity Index
TEM	Transmission Electron Microscopy
TGA	Thermo Gravimetric Analysis

INTRODUCTION

A $W_1/O/W_2$ double emulsion may be an advantageous system for drug encapsulation and controlled release of chemical species initially entrapped in the internal droplets (1). For imaging, it is of interest to develop systems capable to control the pharmacokinetics of contrasting agents (2). New self-emulsifying multiple $W_1/O/W_2$ nanoemulsions were recently developed to vectorize hydrophilic compounds, and they were found to exhibit no cytoxicity (3). The interest of the formulation is to present a granulometric profile with droplet size of the multiple droplets in the nanometric size range, thus allowing parenteral administration (4). The self-emulsifying

process presents a second interest to the formulation because the emulsion is obtained without the need for high energy either mechanic or thermal, thereby limiting the risk of destruction of the W_1/O droplets during the second emulsification step and allowing the inclusion of sensitive compounds.

In addition, the double emulsion allows co-inclusion of both hydrophilic and lipophilic drugs (5). This property, implying the possible simultaneous inclusion of therapeutic and contrast agents (6), would be advantageous in theranostics. Self-emulsifying emulsions were mainly developed for therapeutic purposes and for oral delivery (7), and there are few examples of multiple emulsions with droplet size ranges in the nanometric scale, although it allows intravenous administration (8). Magnetic resonance imaging (MRI) is a non-invasive method whose sensitivity can be increased with contrasting agents. For this purpose, several nanosystems, such as micelles (9,10), microspheres, nanoparticles, liposomes (11–13) and, niosomes (14) have been previously developed as carriers of gadolinum chelates, such as diethylenetriaminepentaacetic-Gadolinum (DTPA-Gd), a positive MRI contrast agent used in clinical practice nearly for two decades. Main drawback of these formulations would be low encapsulation efficiency, complex process of formation and limited stability. The main advantages of a nanoemulsion as a drug carrier over other nanotechnologies, including liposomal formulations, are high loading capacity, formulation stability and ease of manufacture (15).

To the best of our knowledge multiple (double) nanoemulsions have not yet been developed as positive MRI contrast agents bearing gadolinium chelates. In the field of imaging, multiple emulsions were more likely developed as microbubbles to improve ultrasound contrast (16). This formulation could however improve the MRI contrast signal, and allow to further develop a platform for imaging, as it has been developed for iron oxyde O/W nanoemulsions (17). The purposes for this work were to improve the inital $W_1/O/W_2$ formulation in order to efficiently encapsulate DTPA-Gd using (i) wax (hard fat) to stabilize the oil /water interface of the W_1/O primary emulsion (18,19) (ii) human serum albumin (HSA) in the external water phase W_2 to enhance steric stabilization against flocculation and coalescence (20). On the optimized formulations, the aim was to develop relevant methods (*i.e.* calorimetry and ultrafiltration) to characterize the double system and assess its encapsulation capacity. Differential scanning calorimetry (DSC) has recently been suggested as a powerful method to characterize multiple $W_1/O/W_2$ emulsion (21) but to the best of our knowledge, this method has not been applied yet to characterize a complex system in which the droplets are in within the nanometric scale and are formed by a self-emulsification process. Finally, on the characterized formulations, the aim was to assess the ability of the emulsion to increase the MRI contrast in comparison to the reference DTPA-Gd solution.

MATERIALS AND METHOD

Materials

Polysorbate 85, polyoxyethylene 20 sorbitan trioleate (Montanox® 85) was provided by Seppic (Paris, France). Semi-synthetic glyceride hard fat comprising saturated C8-C18 triglyceride fatty acids with hydroxyl value: 5 (Suppocire® DM) were kindly provided by Gattefossé (St Priest, France), and medium chain C8-C10 triglycerides (MCT) by SIO (St Laurent Blangy, France). Glycerol was provided by Fagron (Colombes, France). Diethylene triamine penta acetic acid (DTPA), Europium (III) and Gadolinium (III) were provided by Sigma-Aldrich (Lyon, France). Human Serum Albumin (HSA) (Vialebex® 200 mg/ml) was provided by LFB (Alès, France). All other reagents were of pharmaceutical grade.

The Formulation and Preparation of Self-Emulsifying $W_1/O/W_2$ Nanoemulsions

The optimization of our previous formulation (3) was performed by substituting a part of the lipid phase with semi-synthetic glyceride hard fat, which solidifies at ambient temperatures and thus stabilizes the multiple oil droplets. Moreover, HSA was introduced into the water external phase in order to improve the interfacial stabilization of the droplets as it was known that protein are able to give thermodynamically and kinetically more stable emulsions (22,23).

Multiple $W_1/O/W_2$ nanoemulsions were prepared using a two-step emulsification process: a first step to form the primary emulsions (W_1/O) and a second one to form the multiple nanoemulsions ($W_1/O/W_2$), as previously described (3). Briefly, a blend of oil and surfactants was firstly mixed with a high shear mixer (Ultra-Turrax® T 25 basic, Ika-Werke, Staufen, Germany) at 13 500 rpm for 15 min. The W/O primary nanoemulsions were formed by admixing water with oil and surfactant blend with gentle vortex stirring to ensure thorough mixing. The previous W/O nanoemulsion was directly added to water with a weight ratio nanoemulsion/water of 1:2.

Self-emulsifying $W_1/O/W_2$ Nanoemulsion Characterization and Drug Encapsulation Efficiency

To ease the characterization of the $W_1/O/W_2$ nanoemulsions, a lanthanide series chelate, europium, was used as an analogue for the widely used MR contrast agent gadolinium. Eu and Gd, which are neighboring elements on the periodic table, share many fundamental properties, including ionic radius, valence, and chemical reactivity. But in contrast to Gd, Eu is easier to detect due to its fluorescence properties (24). DTPA-Eu can be detected by time resolved fluorimetry (25) which represents an excellent model of DTPA-Gd MRI contrast agent.

Particle Size, Zeta Potential and pH

The mean multiple droplet size (MDS) and polydispersity index (PDI) of multiple droplets were determined by dynamic light scattering (DLS) (Zetasizer Nano-SZ®; Malvern Instruments Ltd, Malvern, UK) as previously described (3). The PDI is a dimensionless measure of the width of the size distribution, calculated from the cumulant analysis ranging from 0 to 1. A small value of PDI, usually 0.2, is indicative of a monodisperse population. The zeta potential was obtained from electrophoretic mobility measurements using a Zetasizer Nano-SZ® (Malvern Instruments Ltd) as previously described (3). The pH of the formulations was measured using Seven Compact™ pH/ion meter S220 (Mettler-Toledo International Inc., Columbus, OH, USA) at 25°C.

The short term stability of the multiple nanoemulsion was assessed after 30 days of storage at room temperature (25°C) by visual observation and by measuring MDS and PDI.

Transmission Electron Microscopy (TEM)

The multiple $W_1/O/W_2$ emulsions were observed by TEM with negative coloration with a JEOL JEM 2100 (JEOL Ltd, Tokyo, Japan), as previously described (3). TEM was operating at 200 kV and magnifications of × 20,000 × 40,000, and × 100,000. Images were recorded using a 2 k Ultrascan® 1000 CCD Gatan camera (Gatan Inc, Pleasanton, CA, USA).

Ultrafiltration

Encapsulation efficiency (E.E.) of drugs into the $W_1/O/W_2$ system was determined by using an ultrafiltration method adapted from Gan *et al.* (26), using centrifugal filter tube (Amicon Ultra, Ultracel-3 K, Millipore, Ireland) with a 3000 Da cut-off. Three mL of the compound-loaded nanoemulsions were introduced into the filter tube and one unique centrifugation cycle was applied for 30 min, 4500 rtpm at 25°C. The amount of encapsulated drug was calculated by measuring the difference between the total amount of the drug used to prepare the emulsion and the amount of drug that remained in the aqueous phase after isolating the external water phase and the W_1/O primary emulsion, applying the equation from Gan *et al.* (23). The measurement of the europium signal was performed by time-resolved fluorescence at 616 nm with a spectrofluorimeter (Wallac 1420 Victor2, Perkin Elmer). Measurements were done in triplicate. Additionally, recovery experiments were performed to validate of the method.

To assess the recovery of the drug by ultrafiltration, reference solutions with low concentrations of DTPA-Eu (1 and 3 mM) first, then solutions with higher concentrations (10 and 50 mM) were simultaneously filtered with an unloaded emulsion. The recovery was compared to the filtered DTPA-Eu reference water solution. The recovery was calculated according to $R = Cd/Ct \times 100\%$, where Cd is the europium concentration detected in the filtrate, and Ct is the theoretical amount added.

Potential interaction with polysorbate 85 surfactant was assessed by recovering of a DTPA-solution (3 mM) when it was mixed with the surfactant after an ultrafiltration/centrifugation cycle. Additionally, the possible formation of a polydispersed system was assessed by DLS on filtrate and upper part of the filter after an ultrafiltration/centrifugation cycle.

Thermal Analysis

The Differential Scanning Calorimetry (DSC) experiments were achieved using a differential scanning calorimeter 822e (Mettler-Toledo, Switzerland) calibrated beforehand with high purity indium ($T_{fus} = 156.6$°C, and $\Delta_{fus}H = 28.45$ J.g^{-1}) and zinc ($T_{fus} = 419.6$°C, and $\Delta_{fus}H = 107.5$ J.g^{-1}). Thermogravimetry analysis (TGA) was carried out with a TGA 851 (Mettler-Toledo, Switzerland). DSC and TGA runs were performed at 1 or 2°C.min^{-1} under an atmosphere of dry nitrogen gas. Before each DSC experiment, a fresh multiple emulsion sample was introduced in a hermetically closed aluminum pan which was then opened on the top by means of a hole of controlled size (0.7 mm). The multiple emulsions were first studied by cooling the sample from 25 to −80°C, then by heating it from −80 to 25°C. In order to understand the behavior of the multiple emulsions upon heating and in order to highlight the internal water phase DSC signal, the external water phase was evaporated from 25 to 300°C at 2°C.min^{-1}thanks to the thermogravimetric experiments performed. The evaporation profile as a function of the temperature allowed evaporating the external water phase (W_2) while monitoring the DSC endothermic signal of the evaporation of water. Once the total amount of the external water was evaporated, the pan was immediately quenched at room temperature, and then cooled from 25 to −80°C. The thermograms thus obtained present only the internal water phase (W_1) and the mixture of oil and surfactants of the W_1/O primary emulsion endothermic signals. The encapsulation efficiency was estimated by comparing the signals relative to the evaporated external water of the multiple emulsions with and without the DTPA-Eu in W_1 phase.

MRI Experiments

Purification of Nanoemulsions

Prior to MRI experiments, nanoemulsions were purified using ultrafiltration method to remove the potential amount of free drug (not encapsulated) in W_2 phase. For validation of the purification methods, the previous ultrafiltration method was

applied but with gentle conditions of centrifugation of 15 min 4600 rtpm at 25°C. At the end of each centrifugation cycle, all the W_2 phase extracted was removed and analyzed for fluorimetric detection. Measurement of the europium signal was performed by time-resolved fluorescence at 616 nm with a spectrofluorimeter (Wallac 1420 Victor2, Perkin Elmer). Measurements were done in triplicate. The amount of extracted aqueous phase was compensated in the emulsion phase with an equal volume of water introduced in the nanofilter. The number of ultrafiltration/centrifugation cycles necessary to extract non-encapsulated DTAP-Eu was determined, and the same number of cycles was applied for purification of loaded DTPA-Gd W/O/W nanoemulsion for MRI experiments.

MRI Protocol

The MRI experiments were carried out at a magnetic field of 7T. A 7T MR imaging vertical spectrometer was fitted with an ultra shielded refrigerated magnet (300WB, Bruker, Avance II, Wissembourg, France), and equipped with a nominative 200 mT/m actively shielded gradient coil and Paravision 5 acquisition software.

For *in-vitro* relaxivity experiments, T_2 and T_1 maps were recorded at 298 K. The parameters were as follows: for T_2 map, multi echo SE images: hermitian pulse 2000 μs/1236 μs 90°/180°, TR/TE = 15 s/11 ms, 32echos, for T_1 quantitation, saturation RARE images TR = 15 s, 8 s, 3 s, 1.2 s, 0.8 s, 0.6 s, 0.3 s, 0.15 s, 0.050 s, 0.033 s, RARE factor 4. We used: FOV = 4 × 4 cm, matrix size = 128 × 64, 1 slice, 1.5 mm thickness. T_1 and T_2 relaxation times of samples with 0.05, 0.1, 0.5 and 1 mM Gadolinium were quantified by relaxation time T_1 and T_2 fitting. The molar relaxivities r_1 and r_2 were obtained from the slope of the linear fit of the measured T_1-values and T_2-values as a function of the gadolinium concentration. The relaxivity r_1 is given by $1/T_1 = 1/T_{10} + ri_1$ [Gd3+] and r_2 in $mM^{-1}.s^{-1}$ were computed using excel software.

Determination of the Amount of Gadolinium in Multiple Nanoemulsion by Inductively Coupled Plasma Absorption Emission Spectroscopy (ICP-AES)

The amount of Gadolinium incorporated into the multiple nanoemulsion was determined by inductively coupled plasma mass spectrometry (ICP-MS). Multiple $W_1/O/W_2$ emulsions were loaded Gadolinium (III) at 0.05, 0.1, 0.5 and 1 mM of final concentration. Control of the final concentration by ICP-AES was determined after a 1:100 dilution of the samples in 2% $HN0_3$ according to a calibration curve of $GdCl_3$ in presence of empty emulsion treated similarly to the samples of interest. The Gd values were used to evaluate the real relaxivity.

Statistical Analysis

One-way ANOVA and Dunett's multiple comparison tests were performed to compare the characteristics and encapsulation efficiency of the formulations (GraphPad Software, Inc., La Jolla, CA 92037 USA).

RESULTS

Formulation of $W_1/O/W_2$ Nanoemulsions

A first $W_1/O/W_2$ nanoemulsion was optimized and evaluated in terms of cytotoxicity (3). For this formulation, in our previous work (3) no cytotoxicity was detected by Alamar Blue (AB) test both after 1 h and 24 h of incubation with undeterminable IC50 values. Moreover apoptotic mechanisms were not evidenced by chromatin condensation and P2X7 cell death receptor activation tests. In this study, the stability of this first formulation was tentatively improved by the addition of semi-synthetic glycerides wax in the oil phase and/or Human Serum Albumin (HSA) in the external water phase (W_2). Moreover, the volume of the internal phase was increased in order to improve the encapsulation efficiency. Compositions of the investigated nanoemulsions are given in Table I for the primary W_1/O nanoemulsions and Table II for the multiple $W_1/O/W_2$.

Characterization of the Multiple Nanoemulsions

Transmission Electron Microscopy

Double emulsion was identified with negative coloration transmission microscopy. Formulations showed a multiple system by inclusion of water droplets in oil vesicles (Fig. 1), Figure 1 shows TEM micrographs of multiple nanoemulsions with Fig. 1a $W_1/O/W_2$ nanoemulsions including HSA in W_2 phase, Fig. 1b $W_1/O/W_2$ nanoemulsions including wax in the oil phase of the primary W_1/O nanoemulsion and Fig. 1c including both HSA and wax. No difference was observed between the formulations tested in terms of electron microscopic images. The encapsulation of the drug did not show any difference in the electron microscopic images.

Table I Composition (% w/w) of the Primary W_1/O Nanoemulsions

Formulation	Control	(b)wax
Polysorbate 85	13.3	13.3
Glycerol	31.1	31.1
Oil : (Medium Chain Triglyceride)	35.6	17.8
Wax (Suppocire® DM)	-	17.8
Water (W_1)	20	20

Table II Composition (% w/w) of the Multiple $W_1/O/W_2$ Nanoemulsions

Formulation	Control	(a)HSA	(b)wax	(c) HSA & wax
Primary W_1/O emulsion	33	33	33	33
Water (W_2)	67	–	67	–
Water (W_2) including 5% HSA	–	67	–	67

Particle Size Distribution and Zeta Potential

Using one-way ANOVA and Dunett's multiple comparison test, no difference was found at D_0 between the control formulation and a formulation including 5% HSA with regards to Mean Droplet Size (MDS) (Table III), whereas when wax was included, in combination or not with HSA, the MDS were significantly lower than the control $p<0.001$. All polydispersity indexes (PDI) were below 0.2 showing monodisperse granulometric repartition of the multiple droplets. Zeta potential was significantly ($p<0.05$) more negative when either HSA, wax or both was added in the formulation.

Characterization (Size, Zeta Potential, pH) of the Formulations when Loaded with DTPA-Eu

DTPA-Eu was used as a model compound for Gadolinium chelate (DTPA-Gd) MRI contrast agent. When DTPA-Eu was included in the formulation (Table IV), a slight but significant increase of the mean droplet size was observed for all formulations except for the one combining HSA and wax. No significant differences were observed for polydispersity indexes with or without contrast agent. All PDIs were below 0.2 and showed monodisperse granulometric repartition, with or without contrast agent. When DTPA-Eu was added, all the formulations were more negative than the corresponding formulations without contrast agent. In comparison to the control loaded formulation, zeta potential was less negative with HSA or wax alone, but no difference in zeta potential was found between control formulation and the formulation combining wax and HSA. When DTPA-Eu was loaded, the pH was globally increased for the most acid formulations (control and b) (Table IV) and was close to neutrality when HSA was included in the formulation.

Short-term Stability of $W_1/O/W_2$ Nanoemulsions

No difference in the macroscopic aspect of the multiple emulsions has been noticed during the 1-month observation. Comparison of the MDS from $W_1/O/W_2$ formulations at D_0 and D_{30} are shown in Fig. 2. At D_{30}, all MDS were significantly ($p<0.0001$) higher than their corresponding MDS at D_0. At D_{30}, in comparison to the control, MDS were significantly higher for the formulations including HSA 5% and significantly lower for the one including wax only. PDI were lower than 0.2 at D_{30} for all formulations **e**xcept the one combining HSA and wax, in which PDI was just above with 0.260 ± 0.015.

When comparing MDS between D_0 and D_{30}, all formulations exhibited significantly higher MDS ($p<0.0001$) at D_{30}. The lowest MDS was obtained with the formulation including wax only.

Thermal Analyses

To ensure that the nanoemulsions observed by TEM were indeed multiple emulsions, thermal analyses were carried out. As a matter of fact, DSC experiments carried out on cooling $W_1/O/W_2$ nanoemulsions do not allow to differentiate the internal water phase from the external water phase, as already observed for microemulsions (21,27) for instance. This can be explained by the fact that W_1 and W_2 simultaneously crystallizes upon cooling. Consequently, in an attempt to observe the corresponding signal of the internal water phase by means of calorimetry, the external water phase of the nanoemulsion was first evaporated by heating the multiple nanoemulsions before freezing them, as is detailed in the Experimental Method section. This was possible since the thermogravimetric experiments carried out on the multiple nanoemulsions have shown that the external water phase

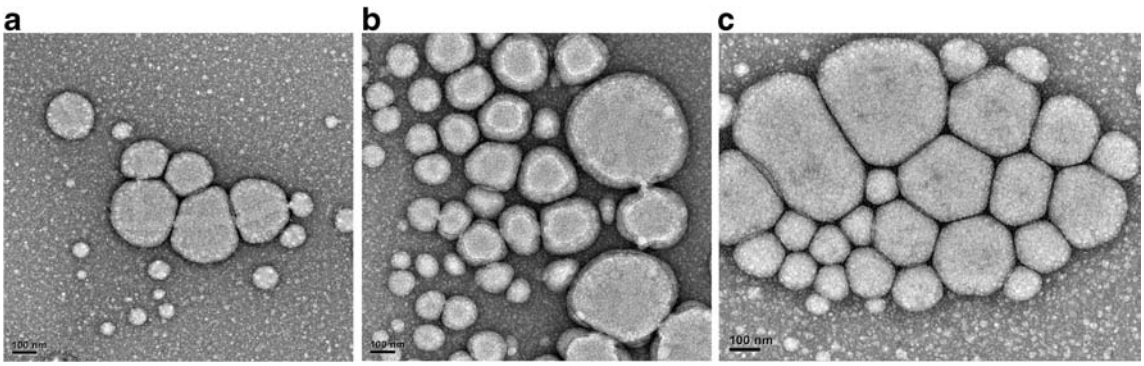

Fig. 1 TEM micrograph of W/O/W nanemulsions including (**a**) HSA (**b**) wax (**c**) Wax and HSA.

Table III Granulometric Results, Zeta Potential, pH of the W/O/W Nanoemulsions at D_0

Formulation	Control[a]	a (HSA)[a]	b (wax)[a]	c (HSA & wax)[a]
MDS (nm)	184.5 ± 1.5	185.4 ± 0.6	174.3 ± 1.9	178.6 ± 0.5
PDI	0.165 ± 0.009	0.169 ± 0.016	0.155 ± 0.010	0.192 ± 0.006
pH	4.3 ± 0.1	6.0 ± 0.1	4.4 ± 0.1	6.6 ± 0.1
Zeta potential	−6.25 ± 0.13	−9.15 ± 0.67	−8.25 ± 1.20	−8.95 ± 0.33

[a] Data are presented as mean value ± standard error ($n = 3$)

slowly evaporates from 25 to 100°C whereas the internal water evaporates at higher temperatures.

The results obtained for the primary W_1/O and multiple $W_1/O/W_2$ nanoemulsions are presented in Fig. 3, and thus allowing a comparison between the DSC signal of each emulsion before (dotted line) and after (solid line) the W_2 phase evaporation.

Upon freezing systems obtained after evaporation present an exothermic signal at lower temperatures, ~ −35°C, as compared to the W_1 crystallization of the primary emulsion which presents upon freezing an exothermic signal at ~ −15°C obtained for the crystallization of water of the multiple nanoemulsions (Fig. 3). Of note, the signal obtained after W_2 evaporation, treated as a function of the sample temperature, is isothermal, unlike to the signal obtained for the $W_1/O/W_2$ nanoemulsion. This indicates that the recrystallization of the external water phase of the multiple nanoemulsions is a very fast phenomenon with a very fast energetic release, inducing a warming of the material (*i.e.* a temperature increase). This phenomenon, which is not observed upon the freezing of the W_1/O emulsion, clearly demonstrates that the W_1 system is encapsulated within the oil phase (confinement effect).

Encapsulation of the Contrast Agent

Encapsulation efficiency was evaluated by ultrafiltration and quantitatively assessed by calorimetry.

Ultrafiltration

Encapsulation efficiency of DTPA-Eu, which was determined by ultrafiltration of three independent experiments, is given in Table V.

We found that introducing HSA in the external phase reduced the encapsulation efficiency in a concentration dependent manner. In contrast, wax introduction in the formulation significantly improved the encapsulation efficiency.

At that stage, it was suspected some interactions with excipients. To investigate this possibility we assessed the recovery of a known amount of DTPA-Eu not included in the emulsion.

DTPA-Eu reference water solution (3 mM) freely passed through the ultrafilter and gave a nearly 100% (99.17%) recovery (Table VI). However, when the solution was mixed with empty $W_1/O/W_2$ nanoemulsions, it was observed that free DTPA-Eu was retained by the filter, and to a larger extent when the emulsion did not include HSA in the external water phase

Retention was concentration-dependent, as was shown on additional recovery experiments involving increasing concentration of DTPA-Eu ultrafiltered with unloaded emulsion (b). Recoveries found were 35, 65 and 96% for the 1, 10 and 50 mM DTPA-Eur concentrations, respectively. The possibility that polysorbate 85 was involved in the interaction was assessed by studying the recovery of DTPA-Eu, after ultrafiltration in a water solution of Polysorbate 85 at the same final concentration as the emulsion. Before ultrafiltration, polysorbate 85 solution exhibited the same fluorescence as the corresponding DTPA-Eu water solution indicating the absence of any quenching phenomenon. After ultrafiltration, the recovery was very low (25%) similar in that to the results obtained with unloaded emulsion (33%). The capacity of polysorbate 85 to form an emulsion on its own was confirmed by DLS measurement of the polysorbate solution in water after a cycle of centrifugation/ultrafiltration. The upper part retained by the filter after centrifugation exhibited a MDS of 126.2 ± 5.09 with a PDI 0.419 indicating the presence of a polydispersed system. In the filtrate, no detectable droplets/ particles were measurable. A part of the PS 85 in excess in the water phase or

Table IV Granulometric Results, Zeta Potential, pH of Loaded $W_1/O/W_2$ Nanoemulsions with DTPA-Eu in Internal Water Phase W_1, Final Concentration 0.2 mM at D_0

Formulation	Control[a]	a(HSA)[a]	b(wax)[a]	c(HSA&wax)[a]
MDS (nm)	191.1 ± 2.9	190.1 ± 0.7	179.0 ± 2.1	179.1 ± 1.0
PDI	0.059 ± 0.031	0.160 ± 0.020	0.171 ± 0.018	0.162 ± 0.018
pH	5.10 ± 0.04	6.86 ± 0.05	5.31 ± 0.17	6.41 ± 0.10
Zeta potential	−11.12 ± 0.07	−10.24 ± 1.16	−9.13 ± 0.04	−11.53 ± 0.53

[a] Data presented as mean value ± standard error ($n = 3$)

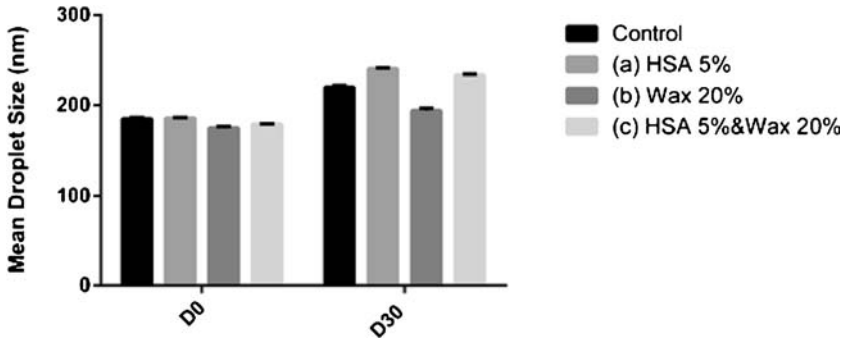

Fig. 2 Mean Droplet size (MDS) comparison at D_0 and D_{30} of the $W_1/O/W_2$ nanoemulsions.

released from the emulsion droplets during the centrifugation stress was able then to form a dispersed system such as a simple emulsion or micelle solution capable to encapsulate free DTPA-Eu.

According to the recovery experiments the encapsulation efficiency may be overestimated due to the risk of interaction of free DTPA-Eu with the excess of free PS85 surfactant in the external water phase. This interaction can be much more important in the case of formulations without HSA. The thermal protocol initially developed to prove that the formation of the multiple nanoemulsions, was used to determine the encapsulation efficiency of DTPA-Eu.

Calorimetry

Experiments were conducted on both wax formulation (Formulation b), considered as the best formulation (combination of best stability and best MDS), and the formulation combining wax and HSA (Formulation c), so as to explore the influence of HSA on the encapsulation efficiency. The DTPA-Eu encapsulation efficiency in the nanoemulsion was assessed by comparing the ratio between the crystallization enthalpy of the internal water phase and that of pure water solution, with the ratio between the crystallization enthalpy of the external water phase with that of the DTPA-Eu solution (Fig. 4). The results are reported in Table VII.

For consistency, all the enthalpy calculations were made at the same temperature for each system (*i.e.* with and without DTPA-Eu), calculating both the specific heat of the water and that of the supercooled water according to Eq. 1 (28). For that purpose, the temperature chosen arbitrarily was the temperature of the internal water crystallization, T_2; T_1 corresponding to the freezing temperature of the water solution.

$$\Delta H(T_2) = \Delta H(T_2) + \int_{T_2}^{T_1} C_{p,\ subcooled\ \ water}.dT + \int_{T_1}^{T_2} C_{p,\ \ ice}.dT \tag{1}$$

with $C_{p,\ ice} = 2.369 + 0.130 \times T$ and $C_{p,\ subcooled\ water} \approx 37.688 + 0.085778 \times T + \frac{5.3764 \times 10^5}{T^2} + 3.663 \times \left(\frac{T}{185} - 1\right)^{-1}$

where ΔH stands for the enthalpy at a given temperature and Cp, for the heat capacity in $J.mol^{-1}.K^{-1}$. The temperatures are expressed in Kelvin

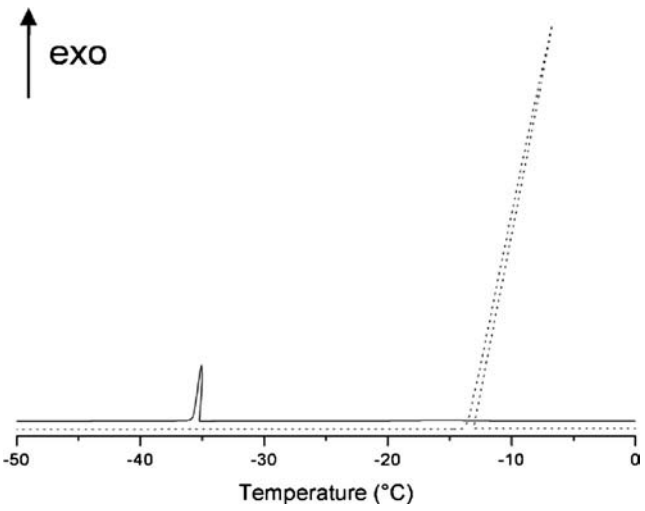

Fig. 3 Weight-normalized DSC thermograms obtained upon freezing of the multiple $W_1/O/W_2$ nanoemulsion (*dotted line*) and the primary W_1/O nanoemulsion (*solid line*). Exothermic transformations give signals pointing up. The thermograms were shifted for clarity.

Table V Encapsulation Efficiency of DTPA-Eu (3 mM) Obtained by Ultrafiltration

$W_1/O/W_2$ nanoemulsion formulations	Encapsulation efficiency (%)	Significance [d]
Control	54.1	–
Control with HSA 0.5%	55.0	NS[e]
Control with HSA 2%	40.0	$p < 0.001$
Control with HSA 5% [a]	12.5	$p < 0.0001$
Wax formulation [b]	59.9	$p < 0.0001$
Wax & HSA 5% [c]	32.8	$p < 0.0001$

[a] Formulation (a)

[b] Formulation (b)

[c] Formulation (c)

[d] One-way ANOVA, Dunett's multiple comparison test in comparison with control (a) formulation

[e] *NS* not significant

Table VI Recovery of DTPA-Eu 3 mM, Final Concentration 0.2 mM

	Recovery %
Reference solution DTPA-Eu 3 mM	99.17
Wax unloaded emulsion[a] + DTPA-Eu 3 mM	33.00
Wax unloaded emulsion including 5% HSA [b] + DTPA-Eu 3 mM	66.00

[a] Formulation (b)

[b] Formulation (c)

The encapsulation efficiency (EE) was calculated with the following equation:

$$EE = \frac{\frac{\Delta H(DTPA - Eu\,loaded\,emulsion)}{\Delta H(DTPA - Eu\,solution)}}{\frac{\Delta H(unloaded\,emulsion)}{\Delta H(pure\,water)}}$$

The encapsulation efficiency of the drug was found to be 69 and 68%, for the wax multiple nanoemulsions prepared with and without HSA, respectively.

MRI

The assessment of MRI contrast was conducted on wax formulation, which was considered as the best formulation (b) with regards to short term stability results, and also on the formulation combining wax and HSA so as to explore the influence of HSA on the MRI contrast (Formulation c).

To assess the relaxivity of only the encapsulated DTPA-Gd, relaxivity studies were performed on purified and non-purified nanoemulsions. Purification was optimized using DTPA-Eu as reported. Six washing cycles were found to be necessary. Purified multiple $W_1/O/W_2$ nanoemulsions (b & c) encapsulated with DTPA-Gd showed a change in contrast of MR images as characterized by their longitudinal relaxivity (r_1 and r_2) evaluated at 7T 298K (Table VIII)

Both wax $W_1/O/W_2$ nanoemulsions with and without HSA in the external water phase exhibited higher r_1 and r_2 relaxivities in comparison to unencapsulated DTPA-Gd. r_1 was similar with and without HSA, whereas r_2 was superior when HSA was included in the formulation which could be rationalized by the decrease of water diffusion near the Gd complex. To create an efficient MR contrast agent of T_1 type by supplying a hypersignal image with this emulsion, the r_2/r_1 ratio should be close to 1. The optimum r_2/r_1 ratio at 1 was obtained with the purified emulsion without HSA. Nevertheless, both nanoemulsions with HSA and without HSA could be considered as a good T_1 type MR contrast agent as shown in Fig. 5.

DISCUSSION

A previously formulated self-emulsifying $W_1/O/W_2$nanoemulsion showing no effect on cell viability (3), was optimized to include a contrast agent into the W_1 internal water phase.

Formulation

In this study, the previously developed formulation (3) showing no toxic effect on cell viability was optimized to increase the stability and improve the encapsulation efficiency. Internal water phase was successfully brought from 10 to 20% w/w of the primary emulsion in order to include more contrast agent inside the internal W_1 phase. In contrast to Schuch *et al.*, (29) the increased concentration of internal water phase (W_1) did not compromise the stability of the double nanoemulsion. This may be explained by the use of the polysorbate 85 surfactant which, compared to other surfactants, is able to absorb a larger mass of water with lower surfactant concentration and also produce finer particles (30).

Wax coming from semisynthetic glycerides was shown to stabilize small size nanoemulsions by reducing the Ostwald ripening efficiency at 10% w/w or above (31). Wax addition in the primary emulsion was successfully achieved. According to our results, wax was able to improve both the stability of the system and the encapsulation efficiency.

Human serum albumin was added into the external W_2 water phase based on the principle that proteins yield thermodynamically and kinetically more stable emulsions (22,23).

Table VII Thermodynamic Data Deduced From the DSC Results for Water, DTPA-Eu Solution, Multiple Wax $W_1/O/W_2$ Nanoemulsion and W_1/O Primary Emulsion Prepared Without and With HSA

	T_1 (K)	$\Delta H(T_1)$ (kJ.mol^{-1})	$\Delta H(T_2 = 236$ K) (kJ.mol^{-1})	$\Delta H(T_2 = 238$ K) (kJ.mol^{-1})	Encapsulation efficiency
Pure water	260	−5.52	−4.56	−4.55	–
0.6 mM DTPA-Eu solution	258	−5.48	−4.51	−4.60	–
unloaded emulsion without HSA	239	−5.89	–	−5.84	68%
DTPA-Eu loaded emulsion without HSA	–	–	–	−4.02	
unloaded emulsion with HSA	238	−4.38	−4.28	–	69%
DTPA-Eu loaded emulsion with HSA	–	–	−2.92	–	

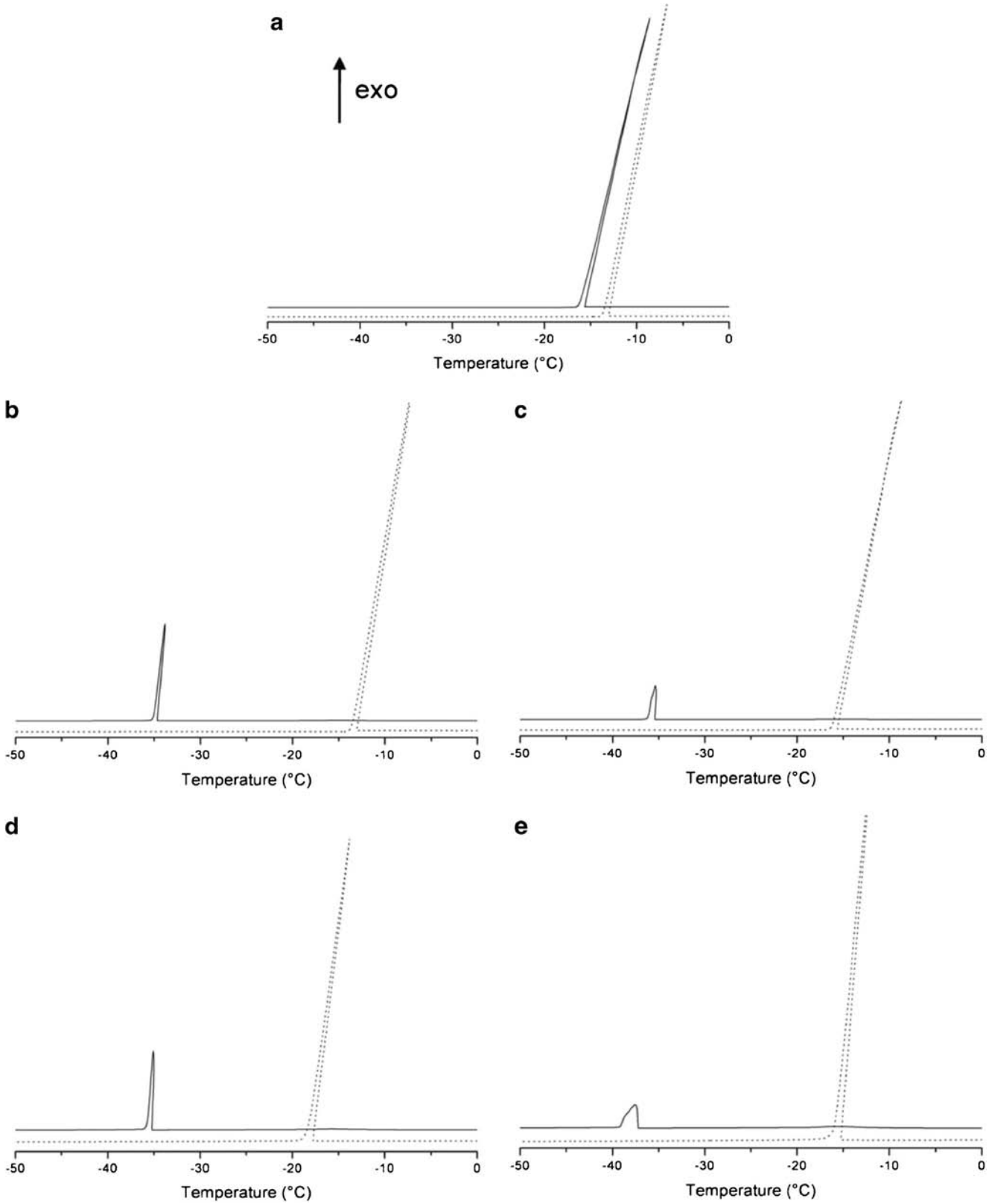

Fig. 4 Weight-normalized DSC thermogram obtained upon freezing. (**a**) Pure water (*dotted line*) and DTPA-Eu solution (solid line). (**b**, **d**) wax $W_1/O/W_2$ (*dotted line*) and W_1/O emulsions (*solid line*) prepared with pure water. (**c**, **e**) $W_1/O/W_2$ (*dotted line*) and W_1/O emulsions (*solid line*) prepared with DTPA-Eu solution. DTPA-Eu solution. The emulsions was prepared without (**b**-**c**) and with HAS (**d**-**e**). Exothermic transformations give signals pointing up. The thermograms were shifted for clarity.

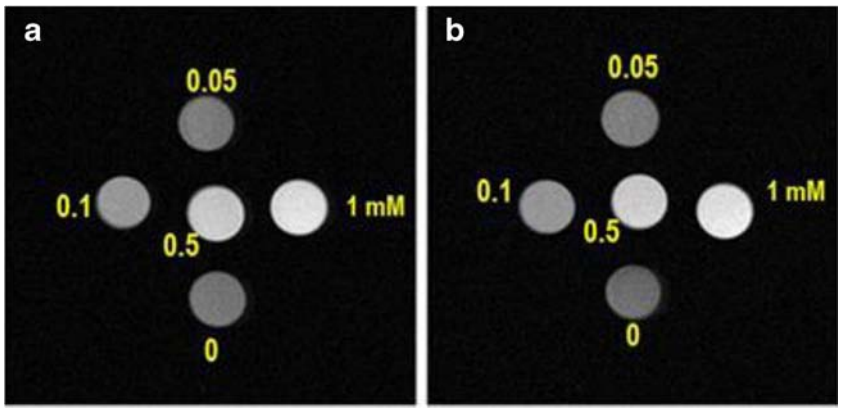

Fig. 5 T1 weighted MRI image at 7T of the nanoemulsions (**a**) without HSA, (**b**) with HSA at different Gd concentration (0, 1 to 1 mM).

With regards to stabilization, no improvement was obtained when HSA was included in the formulations. Moreover, encapsulation efficiency was not improved either. For our double nanoemulsions our results showed that there was only minimal interest to add HSA into the W_2 external water phase of the emulsion.

Characterization

Characterization of self-emulsifying nanomultiple systems was quite challenging, due to the nanometric size and to the self-emulsifying system.

It was already possible to visualize internal water droplets by transmission electron microscopy, but the definitive proof came from thermal analysis. Thanks to our optimized protocol, we were able to differentiate the inner and outer water phases, which gives different crystallization temperatures. Differential scanning calorimetry (DSC) has recently been suggested as a powerful method to characterize multiple $W_1/O/W_2$ emulsions (21). However, to the best of our knowledge, characterization of self-emulsifying multiple nanoemulsions by DSC has not been described yet. Many publications report thermal characterizations of microemulsions (21,27), often achieved either upon freezing or upon freezing/melting. On the basis of these experiments, it is now possible to differentiate, for instance, the behavior of the encapsulated water relative to the external phase. On freezing, when external water crystallizes between −10 and −20°C, the inside water phase crystallizes at temperatures lower than −30°C, depending on the size of the droplets (32). Once the external bulk water phase crystallizes, it has been reported that water transfer may occur from the droplets to the bulk water phase (21,33). This phenomenon may be observed on the DSC thermograms by a shoulder forming after the crystallization peak. This mass transfer can be partial or complete, depending on the experimental conditions. It has also been proposed that crystallization of the bulk water phase could cause the crystallization of the internal water phase. Whatever the explanation, it may lead to the non-observation of DSC signals for the crystallization of the internal water phase, upon cooling. It was demonstrated that multiple nanoemulsions can be characterized by DSC and TGA. In addition to this, it was demonstrated that it is possible to distinguish the internal water phase signal from the external water phase signal by DSC. Besides, the DSC signals obtained for the W_2/O emulsions prepared with DTPA-Eu present a different shape from those obtained for the W_2/O emulsions prepared with pure water. The phenomenon is more pronounced when the DTPA-Eu is associated with HSA.

Table VIII MR r_1 and r_2 Values of Purified $W_1/O/W_2$ Wax Nanoemulsions Loaded with DTPA-Gd in Comparison with DTPA-Gd Solution

$mM^{-1}.s^{-1}$	r_1	r_2	r_2/r_1
DTPA Gd solution	3.9	4.1	1.05
$W_1/O/W_2$ nanoemulsion without HSA (b)	6.0	6.0	1.00
$W_1/O/W_2$ nanoemulsion with HSA 5% (c)	5.9	21.6	3.14

Encapsulation Efficiency Determination

The most commonly used contrast agent for Magnetic resonance imaging is DTPA-Gadolinium (DTPA-Gd) complex. To improve the characterization of the $W_1/O/W_2$ nanoemulsions, europium was used as an analogue for Gadolinium. Indeed, due to their proximity in the periodic table, Eu and Gd have similar physical properties, but in contrast to Gd, Eu is easier to detect due to its fluorescence properties (24). DTPA-Eu can be detected by time-resolved fluorimetry (25), which represents an excellent model of DTPA-Gd MRI contrast agent.

Since the studied system is self-emulsifying, it was a challenge to determine the encapsulation efficiency of the drug. Using ultrafiltration/centrifugation method, the use of very low cut off of 3 kDa has been necessary to retain W_1/O primary emulsion. Considering the recovery experiments on unloaded emulsions, interactions were revealed with free DTPA-Eu and HSA. Interaction with free DTPA-Eu in the

solution can be attributed to the polysorbate 85 surfactant which is known to have a limited capacity to encapsulate water-soluble drugs and to form a self-emulsifying emulsion (30). Moreover, polysorbate 85 can be involved in interactions with proteins, as previously described (34). The interactions revealed by the recovery experiments showed some limitations to the assessment of the encapsulation efficiency by ultrafiltration. At this stage the DSC method was of higher interest to control the results obtained by ultrafiltration. In fact, DSC showed encapsulation efficiency similar to ultrafiltration results except when HSA was in the formulation, where the encapsulation efficiency was underestimated by ultrafiltration. According to our results, the encapsulation efficiencies were quite high with 68% encapsulated DTPA-Eu in the wax formulation.

MRI of DTPA-Gd $W_1/O/W_2$ Nanoemulsions

MRI is one of the most powerful diagnosis technique for molecular imaging. However, it is limited in terms of sensitivity because both healthy and pathological tissues show similar magnetic moments, thus producing poor image contrast. To overcome this limitation paramagnetic positive contrast agents such as Gd(III) chelates (35) are commonly used in clinical MRI, because they and allow a uniform distribution to all perfused tissues and into extracellular spaces. Free Gd (III) is toxic, which is why it has to be chelated to a ligand such as DTPA(35). To improve the targeting of the contrast agent to a specific site such as a tumor, targeted nanoparticles such as liposomes (11–13) and micelles (9,10) including gadolinium complex, have been developed. In agreement to our results, we found from *in vitro* relaxivity studies that the $W_1/O/W_2$nanoemulsions loaded with DTPA-Gd were able to increase the positive contrast (r_1=6 $mM^{-1}.s^{-1}$) when compared with the experimentally found DTPA-Gd solution (r_1=4 $mM^{-1}.s^{-1}$). Relaxivity of the DTPA-Gd solution was similar to previously published data, as in Hak *et al.* (12). The relaxivity r_1=6 $mM^{-1}.s^{-1}$ of the $W_1/O/W_2$ nanoemulsions was higher than the relaxivity found in the literature with loaded DTPA-Gd particles (2) and was better than that of liposomes (36,37). In liposomes, the lower relaxivity has been explained by a reduced kinetics of the proton exchange rate between external H_2O and encapsulated Gd chelate (38) due to a lower water permeability of the bilayer. The r_1 value obtained from 6 mM^{-1} s^{-1} with multiple emulsions at ambient temperature is similar to the liposomal formulation studied at a higher temperature of 45°C (13,39). The reason for this may be due to the need of fluidification of the liposomal bilayer which was obtained by increasing the temperature. Regarding our system and, quite interestingly, at ambient temperature, the water exchange would be facilitated due to the lack of a lipid bilayer in emulsion, due to the fluid phase of the droplet which is known to be more permeable to water (40). Drug movement from W_1 to W_2 can also occur simply via diffusion through the oil membrane without coalescence (41), Ostwald ripening or W_1/O droplet breakdown whereas the liposome bilayer needs fluidification by means of increased temperature.

The ratio r_2/r_1 was close to 1 when HSA was not included in the formulation, but it was over 3 when HAS was included, which could be less favorable for a T_1-type contrast agent as r_2 increased to 21.6 in presence of HSA. The HSA in the external water phase could possibly limit water exchanges by steric stabilization of the oil droplets (20) or contribute to the outer sphere effect due to the limitation of water diffusion near the Gd Complex in presence of HSA.

CONCLUSION

Nanoemulsions obtained by the self-emulsifying process are complicated systems that have been hardly characterized due to their constant equilibrium between formed and unformed emulsions. In this study, $W_1/O/W_2$ nanoemulsions have been sufficiently stabilized to elaborate reliable methods of characterization. Upon wax incorporation, it was evidenced the formation of a $W_1/O/W_2$ nanoemulsion thanks to an optimized DSC protocol. Applying this protocol to drug encapsulation, the encapsulation efficiency could be quantitatively determined, thus confirming ultrafiltration results which also had to be optimized to avoid artifacts. Finally, double $W_1/O/W_2$ nanoemulsions were found to be able to encapsulate MRI contrasting agent with high encapsulation efficiency and to exhibit higher positive contrast than DTPA-Gd solution.

The potentiality of this formulation for theranostic purposes should be evaluated.

ACKNOWLEDGMENTS AND DISCLOSURES

The authors wish to thank Jean-Michel Guigner, Institut de minéralogie et de physique des milieu condensés IMPC-IRD-CNRS UMR 7590, UPMC for his support for TEM imaging and ED387-iViV, UPMC Sorbonne Université, Paris, France for supporting this project.

We thank the Maison des Langues, Université Paris Descartes, Sorbonne Paris Cité, 45 rue des Saints-Pères, 75006 Paris France for their review of the English manuscript.

REFERENCES

1. Pays K, Giermanska-Kahn J, Pouligny B, Bibette J, Leal-Calderon F. Double emulsions: how does release occur? J Control Release. 2002;79:193–205.
2. Doiron AL, Chu K, Ali A, Brannon-Peppas L. Preparation and initial characterization of biodegradable particles containing

gadolinium-DTPA contrast agent for enhanced MRI. Proc Natl Acad Sci U S A. 2008;105:17232–7.
3. Sigward E, Mignet N, Rat P, Dutot M, Muhamed S, Guigner JM, *et al*. Formulation and cytotoxicity evaluation of new self-emulsifying multiple W/O/W nanoemulsions. Int J Nanomed. 2013;8:611–25.
4. Gupta S. Biocompatible microemulsion systems for drug encapsulation and delivery. Curr Sci. 2011;101:174–88.
5. Chuan YP, Zeng BY, O'Sullivan B, Thomas R, Middelberg APJ. Co-delivery of antigen and a lipophilic anti-inflammatory drug to cells via a tailorable nanocarrier emulsion. J Colloid Interface Sci. 2012;368:616–24.
6. Gianella A, Jarzyna PA, Mani V, Ramachandran S, Calcagno C, Tang J, *et al.* Multifunctional Nanoemulsion platform for imaging guided therapy evaluated in experimental cancer. ACS Nano. 2011;5:4422–33.
7. Pouton CW. Formulation of self-emulsifying drug delivery systems. Adv Drug Deliv Rev. 1997;25:47–58.
8. Solans C, Izquierdo P, Nolla J, Azemar N, Garcia-Celma MJ. Nano-emulsions. Curr Opin Colloid Interface Sci. 2005;10:102–10.
9. Gao GH, Lee JW, Nguyen MK, Im GH, Yang J, Heo H, *et al.* pH-responsive polymeric micelle based on PEG-poly(β-amino ester)/(amido amine) as intelligent vehicle for magnetic resonance imaging in detection of cerebral ischemic area. J Control Release. 2011;155:11–7.
10. Nakamura E, Makino K, Okano T, Yamamoto T, Yokoyama M. A polymeric micelle MRI contrast agent with changeable relaxivity. J Control Release. 2006;114:325–33.
11. Mulder WJM, Strijkers GJ, van Tilborg GAF, Griffioen AW, Nicolay K. Lipid-based nanoparticles for contrast-enhanced MRI and molecular imaging. NMR Biomed. 2006;19:142–64.
12. Hak S, Sanders HMHF, Agrawal P, Langereis S, Grüll H, Keizer HM, *et al.* A high relaxivity Gd(III)DOTA-DSPE-based liposomal contrast agent for magnetic resonance imaging. Eur J Pharm Biopharm. 2009;72:397–404.
13. Mulder WJM, Strijkers GJ, Griffioen AW, van Bloois L, Molema G, Storm G, *et al.* A liposomal system for contrast-enhanced magnetic resonance imaging of molecular targets. Bioconjug Chem. 2004;15:799–806.
14. Luciani A, Olivier J-C, Clement O, Siauve N, Brillet P-Y, Bessoud B, *et al.* Glucose-receptor MR imaging of tumors: study in mice with PEGylated paramagnetic niosomes. Radiology. 2004;231:135–42.
15. Sainsbury F, Zeng B, Middelberg APJ. Towards designer nanoemulsions for precision delivery of therapeutics. Curr Opin Chem Eng. 2014;4:11–7.
16. Yang F, Gu A, Chen Z, Gu N, Ji M. Multiple emulsion microbubbles for ultrasound imaging. Mater Lett. 2008;62:121–4.
17. Jarzyna PA, Skajaa T, Gianella A, Cormode DP, Samber DD, Dickson SD, *et al.* Iron oxyde core oil-in-water emulsions as a multifonctional nanoparticle platform for tumor targeting and imaging. Biomaterials. 2009;30:6947–54.
18. Li C, Liu Q, Mei Z, Wang J, Xu J, Sun D. Pickering emulsions stabilized by paraffin wax and Laponite clay particles. J Colloid Interface Sci. 2009;336:314–21.
19. Nepal PR, Han H-K, Choi H-K. Preparation and in vitro–in vivo evaluation of Witepsol® H35 based self-nanoemulsifying drug delivery systems (SNEDDS) of coenzyme Q10. Eur J Pharm Sci. 2010;39:224–32.
20. Bouyer E, Mekhloufi G, Rosilio V, Grossiord J-L, Agnely F. Proteins, polysaccharides, and their complexes used as stabilizers for emulsions: alternatives to synthetic surfactants in the pharmaceutical field? Int J Pharm. 2012;436:359–78.
21. Schuch A, Köhler K, Schuchmann HP. Differential scanning calorimetry (DSC) in multiple W/O/W emulsions. J Therm Anal Calorim. 2013;111:1881–90.
22. Bos MA, van Vliet T. Interfacial rheological properties of adsorbed protein layers and surfactants: a review. Adv Colloid Interf Sci. 2001;91:437–71.
23. Damodaran S. Protein stabilization of emulsions and foams. J Food Sci. 2005;70:R54–66.
24. Elster AD, Jackels SC, Allen NS, Marrache RC. Dyke award. Europium-DTPA: a gadolinium analogue traceable by fluorescence microscopy. Am J Neuroradiol. 1989;10:1137–44.
25. Mignet N, Chermont Q, Randrianarivelo T, Seguin J, Richard C, Bessodes M, *et al.* Liposome biodistribution by time resolved fluorimetry of lipophilic europium complexes. Eur Biophys J. 2006;35:155–61.
26. Gan L, Gan Y, Zhu C, Zhang X, Zhu J. Novel microemulsion in situ electrolyte-triggered gelling system for ophthalmic delivery of lipophilic cyclosporine A: in vitro and in vivo results. Int J Pharm. 2009;365:143–9.
27. Clausse D. Thermal behaviour of emulsions studied by differential scanning calorimetry. J Therm Anal Calorim. 1998;51:191–201.
28. Leyendekkers JV, Hunter RJ. Thermodynamic properties of water in the subcooled region. I. J Chem Phys. 1985;82:1440–6.
29. Schuch A, Deiters P, Henne J, Köhler K, Schuchmann HP. Production of W/O/W (water-in-oil-in-water) multiple emulsions: droplet breakup and release of water. J Colloid Interface Sci. 2013;402:157–64.
30. Pouton CW, Porter CJH. Formulation of lipid-based delivery systems for oral administration: materials, methods and strategies. Adv Drug Deliv Rev. 2008;60:625–37.
31. Delmas T. How to prepare and stabilize very small nanoemulsions. Langmuir. 2011;27:1683–92.
32. Clausse D, Gomez F, Pezron I, Komunjer L, Dalmazzone C. Morphology characterization of emulsions by differential scanning calorimetry. Adv Colloid Interf Sci. 2005;117:59–74.
33. Mezzenga R, Folmer BM, Hughes E. Design of double emulsions by osmotic pressure tailoring. Langmuir. 2004;20:3574–82.
34. Chou DK, Krishnamurthy R, Randolph TW, Carpenter JF, Manning MC. Effects of Tween 20® and Tween 80® on the stability of Albutropin during agitation. J Pharm Sci. 2005;94:1368–81.
35. Laurent S, Henoumont C, Vander Elst L, Muller RN. Synthesis and physicochemical characterisation of Gd-DTPA derivatives as contrast agents for MRI.Eur J. Inorg Chem. 2012;12:1889–915.
36. Tilcock C, Unger E, Cullis P, MacDougall P. Liposomal Gd-DTPA: preparation and characterization of relaxivity. Radiology. 1989;171:77–80.
37. Unger E, Shen DK, Wu G, Fritz T. Liposomes as MR contrast agents: pros and cons. Magn Reson Med. 1991;22:304–8.
38. Fossheim SL, Fahlvik AK, Klaveness J, Muller RN. Paramagnetic liposomes as MRI contrast agents: influence of liposomal physicochemical properties on the in vitro relaxivity. Magn Reson Imaging. 1999;17:83–9.
39. Strijkers GJ, Mulder WJM, van Heeswijk RB, Frederik PM, Bomans P, Magusin PCMM, *et al.* Relaxivity of liposomal paramagnetic MRI contrast agents. Magn Reson Mater Phys Biol Med. 2005;18:186–92.
40. Dekker M. In: Cevc G, editor. Phospholipids handbook. New York: CRC Press; 1993. p. 988.
41. Magdassi S, Garti N. Release of electrolytes in multiple emulsions: coalescence and breakdown or diffusion through oil phase? Colloids Surf. 1984;12:367–73.